

Numerical Tests of a Method for Simulating Electrical Potentials on the Cortical Surface

R. Baker Kearfott, Robert D. Sidman, Diana Joan Major, and C. Denson Hill

Abstract—A mathematical imaging method for simulating cortical surface potentials was introduced at recent neurosciences meetings [1a], [1b], [2] and was applied to elucidate the neural origins of evoked responses in normal volunteers and certain patient populations. This method consists of the solution of an inward harmonic continuation problem and its effect is to simulate data that has not been attenuated and smeared by the skull.

This cortical imaging technique (CIT) is validated by applying it to artificially derived data. Pairs of dipolar sources with different depths and separations are introduced into a spherical conducting medium simulating the head. Scalp potential maps are constructed by interpolating the simulated data between 28 "scalp" electrode positions. Noise is added to the data to approximate the variability in measured potentials that would be observed in practice.

CIT is used in each case to construct potential maps on layers concentric to and within the layer representing the scalp. In several instances when the dipole pair is deep and closely spaced, the sources cannot be separated by the scalp topographical maps but are easily separated by the "cortical" topographical maps. CIT is also applied to scalp-recorded potentials evoked by bilateral median nerve stimulation and pattern-reversal visual stimulation.

INTRODUCTION AND BACKGROUND

NONINVASIVE localization and description of the neural generators of scalp-recorded potentials is a primary goal of electroencephalography. An approach that is used by some investigators is to simulate these generators by theoretical or equivalent sources and treat the problem as an inverse problem where one seeks the theoretical source(s) of measured boundary potentials. The dipole localization method (DLM) is one such approach. In DLM the head is simulated by a layered conducting sphere and the generators of scalp-recorded potentials are simulated by a single dipolar source. The method consists of finding the dipole source for boundary potentials that gives the best least-squares fit between measured and theoretical voltages [3].

Although DLM is easy to implement and gives physically realistic answers in several cases [4]–[6], in many instances the dipole solution represents the superposition of many neuronal units and is, at best, an equivalent source. Examples include the late components of the visual evoked response [7], [8], the N1-P2 complex of responses to auditory stimulation [9], [10], and the P300 response to oddball auditory stimuli. In the first example, potentials are generated for the most part, in layers of the striate cortex. In the second case, depth recordings of these components of the resting AER are compatible with bilateral posterior temporal sources with a dorso-frontal orientation [10].

The P300 component of the AER appears to reflect endogenous processes related to attention, alertness, and cognition, and is probably not generated in localized cortical areas of the brain.

C. C. Wood *et al.* [11] noted that scalp potential fields do not uniquely determine the location and configuration of generators. They, rather, provide "necessary conditions," that any model must satisfy. This reference and other investigations rely on studies of scalp potential distributions to suggest these necessary conditions. Presumably the collection of sources and sinks gives some information about the generators of the data. In practice, scalp topographical maps are usually produced by linear three- or four-point interpolation and exhibited in colorful displays. In certain cases, such as for the N30-P30 component of the response to simultaneous bilateral median nerve stimulation, the scalp maps clearly suggest two superficial (cortical) sources that are tangential to the surface of the brain. However, the scalp topographies for other data, such as the AER and VER cases mentioned above, do not exhibit enough detail to distinguish a deep localized source from a superficial extensive one or single from multiple sources if these sources are deep in the brain.

Part of the reason why topographical potential maps are inadequate for discriminating multiple sources is that the skull so attenuates and smears the scalp-recorded voltages that detail is lost in the interpolated maps. The imaging technique that is developed here does not create data but is, rather, a new way of extracting information from scalp data—information that was obscured by the interpolation procedures used to construct conventional scalp maps.

Mathematically, this "cortical imaging technique" (CIT) is the solution of a harmonic inward continuation problem. The values of a harmonic function (the electric potential) are known on the surface of a volume conductor (the head). Also, these measured boundary values are noisy. The object of CIT is to continue these noisy boundary values harmonically into the interior of the conductor.

This problem is an ill-posed one in the sense of Hadamard—the solution of Laplace's equation does not depend continuously on the boundary data. It is one of a class of problems that includes the Cauchy problem for elliptic equations, the solution of the heat equation backward in time [12], complex analytic continuation [13], and harmonic continuation on half-spaces [14]. By placing restrictions on our problem, it is possible to restore continuous dependence of data and thus obtain physically useful answers. A more general treatment of this procedure can be found in [15].

CORTICAL IMAGING TECHNIQUE

Let the head be simulated by a homogeneous sphere of radius 1.0 as in Fig. 1. Also suppose that N radial dipoles of unit strength are placed on a spherical shell, the "test" surface, of

Manuscript received September 6, 1989; revised April 7, 1990.

R. B. Kearfott, R. D. Sidman, and D. J. Major are with the University of Southwestern Louisiana, Lafayette, LA 70504.

C. D. Hill is with the Department of Mathematics, State University of New York at Stony Brook, Stony Brook, NY 11794.

IEEE Log Number 9042172.

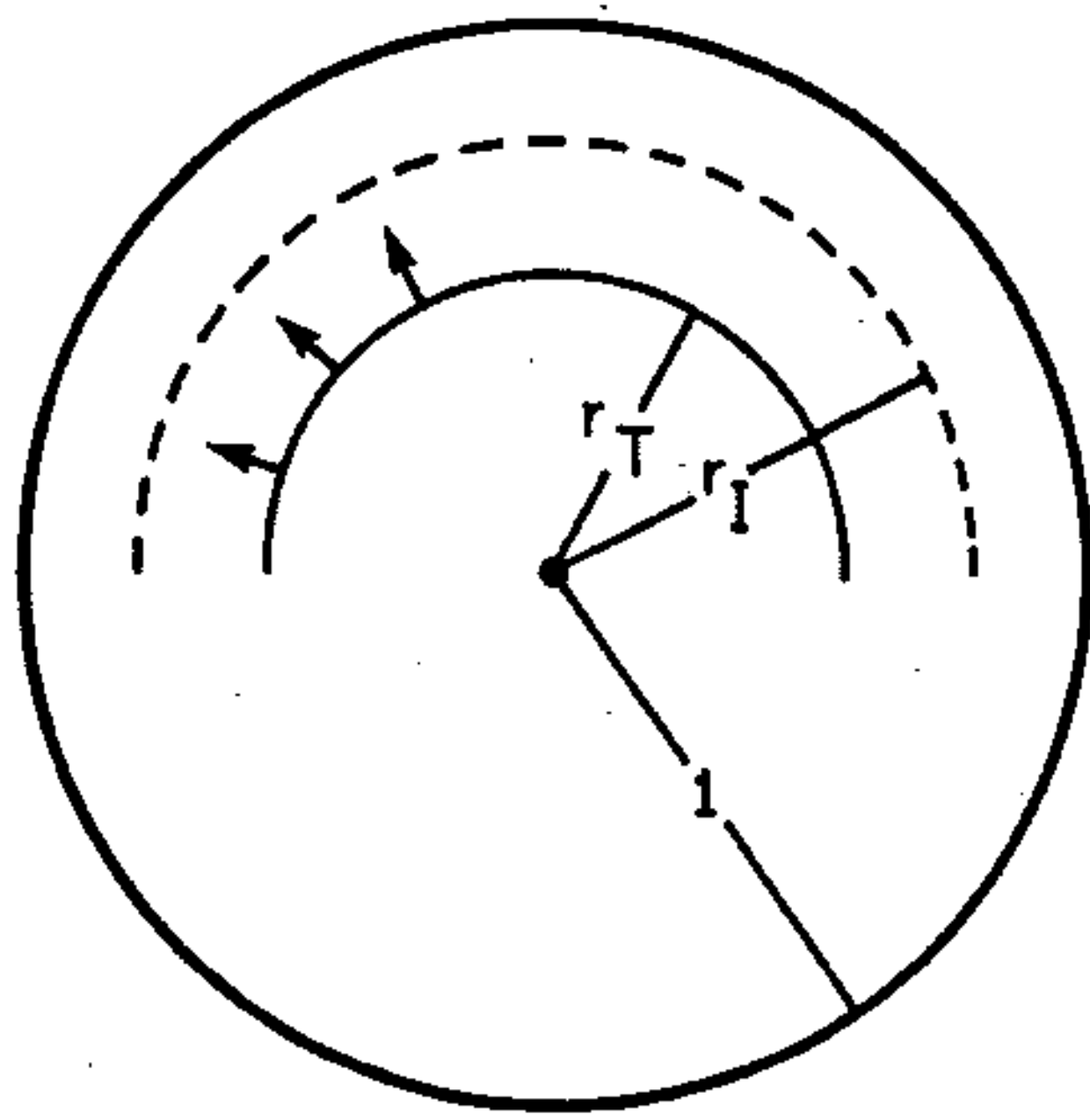


Fig. 1. The "head" is simulated by a sphere of radius 1.0. Test dipoles of unit strength are distributed on a hemispherical shell of radius r_T . Contour plots of the potential generated by the test layer are constructed on a hemispherical shell of radius r_I .

radius r_T . (Throughout this paper, the term "dipole" refers to "current dipole.") This test surface is within and concentric to the surface of the head. A typical dipole of this type D_i is located at Cartesian coordinates $x_i = r_T \cos \theta_i \sin \phi_i$, $y_i = r_T \sin \theta_i \sin \phi_i$, $z_i = r_T \cos \phi_i$, and has moments $\cos \theta_i \sin \phi_i$, $\sin \theta_i \sin \phi_i$, and $\cos \phi_i$, with respect to the coordinate axes. In this paper the x axis passes through the right ear, the y axis goes through the nasion, and the z axis goes through the vertex.

The potential generated by any such dipole can be calculated in the closed form, $V(D_i, P_j)$ where P_j lies within or on the unit sphere simulating the head [16], [17]. These formulas are also given in the Appendix. If V_1, \dots, V_M are voltages measured at scalp recording sites A_1, \dots, A_M , it is certainly possible to calculate weighting numbers u_1, \dots, u_N to satisfy the M equations

$$\sum_{i=1}^N u_i V(D_i, A_j) = V_j, \quad \text{for } j = 1, \dots, M. \quad (1)$$

Generally, $M < N$, so that (1) is an underdetermined system of equations with an infinite number of solutions. However, there is a unique solution that minimizes $(u_1^2 + \dots + u_N^2)^{1/2}$, the L_2 norm of (u_1, \dots, u_N) .

The maximum rank of system (1) is M . In practice, though, the system may be rank-deficient which suggests that the singular value decomposition (SVD) can be used to compute the unique solution of (1) of minimum norm [18]. An additional advantage of the SVD is that it is possible to take account of noise in the data. Given an estimate e_d of the relative errors in the data, one can replace the system (1) by a possibly rank-deficient system such that errors of size e_d will not unduly influence the solution.

In the experimental tests of this technique, described below, test dipoles of unit strength were placed on the test surface, the spherical shell with radius r_T , at positions whose angles in the standard spherical coordinate system were θ_k and ϕ_m , where

$$\theta_k = (k - 1)(2\pi/10), \quad 1 \leq k \leq 10$$

and

$$\phi_m = m(\pi/2)/16, \quad 1 \leq m \leq 16.$$

Hence $N = 160$. With one exception the number of scalp electrode sites in these tests was 28, which were standard 10-20 electrode positions or derivable from them. The exception is the analysis of the response to bilateral median nerve stimulation, where 36 electrode positions are used. Hence, $M = 28$ in all cases except the aforementioned case where $M = 36$.

Once the values u_1, \dots, u_{160} are calculated one can use the principle of superposition and formulas in the Appendix to compute an approximate image of the potential field on any intermediate spherical shell of radius r_I . Note that $r_T < r_I \leq 1.0$. This image surface can include a shell stimulating the surface of the brain. Since the formulas can be used to calculate theoretical potentials at any point of the shell $r = r_I$, topographical scalp maps will be smoother than maps constructed by linear interpolation among only M (28 or 36) points. In the applications discussed below, scalp and "cortical" topographical maps are constructed by interpolating 160 potential values on the grid on $r = r_I$ corresponding to the grid on $r = r_T$ on which the test dipoles D_1, \dots, D_{160} are placed.

We implemented CIT in Fortran-77, and we ran the code on the IBM 3090 at the University of Southwestern Louisiana. The LINPACK routine DSVDC [19] was used for the singular value decomposition. In all experiments with $N = 160$ it took roughly 4 s of CPU time to generate the approximate potential field. We used SAS/GRAPH to generate surface and contour maps.

APPLICATIONS OF CIT TO ARTIFICIALLY GENERATED DATA

The first application of CIT reported here is to the surface potentials generated by the pair of dipole sources

$$(\pm 0.4 \sin(\pi/4), 0, 0.4 \cos(\pi/4), 0, 0, 0.1).$$

The first three entries give the coordinates of the location of the source and the last three entries give its moments (Fig. 2). These sources lie on a shell of radius 0.4 within the "head."

Below this pair of sources in the figure are the three-dimensional perspectives and contour maps of the surface potentials for the actual data and the potentials generated by the optimal dipole layer produced by CIT. In these and subsequent figures the plots are scaled to exhibit approximately 15 equally spaced contours. In this case, $r_I = 1.0$, $r_T = 0.45$, and the "noise ratio" in the SVD is equal to 0.05. The effect of the noise ratio is to change the effective rank of the system (1). This effective rank is the rank of the system obtained by ignoring singular values which are less than 0.05 times the maximum singular value (cf., e.g., [20, Section 5.5]). In this case the effective rank of system (1) is equal to 15, whereas the full rank is 28. Generally decreasing the noise ratio increases the effective rank of the system. In addition, decreasing the noise ratio decreases the maximum relative error between computed and actual electrical potentials, when we are using simulated data. (The maximum relative error is the absolute value of the maximum difference between the true potential and computed potential on the intermediate shell, divided by the maximum absolute value of the actual potential on the intermediate shell, over the grid points used for plotting.)

Note that the figures are indistinguishable and do not exhibit the pair of maxima that would be expected for this pair of sources. However when the "actual" potentials and CIT generated potentials are plotted in Fig. 3 on the image surface $r_I = 0.63$ the multiple sources are clearly distinguished. The graphs of the exact data and the CIT generated potentials are slightly different but the CIT maps preserve the most important feature of the source.

Fig. 4 is a synopsis of the CIT results when 10% noise is added to the surface potentials generated by the preceding pair of dipole sources. (Throughout our tests, we used uniformly distributed pseudo-random noise whose maximum deviation was

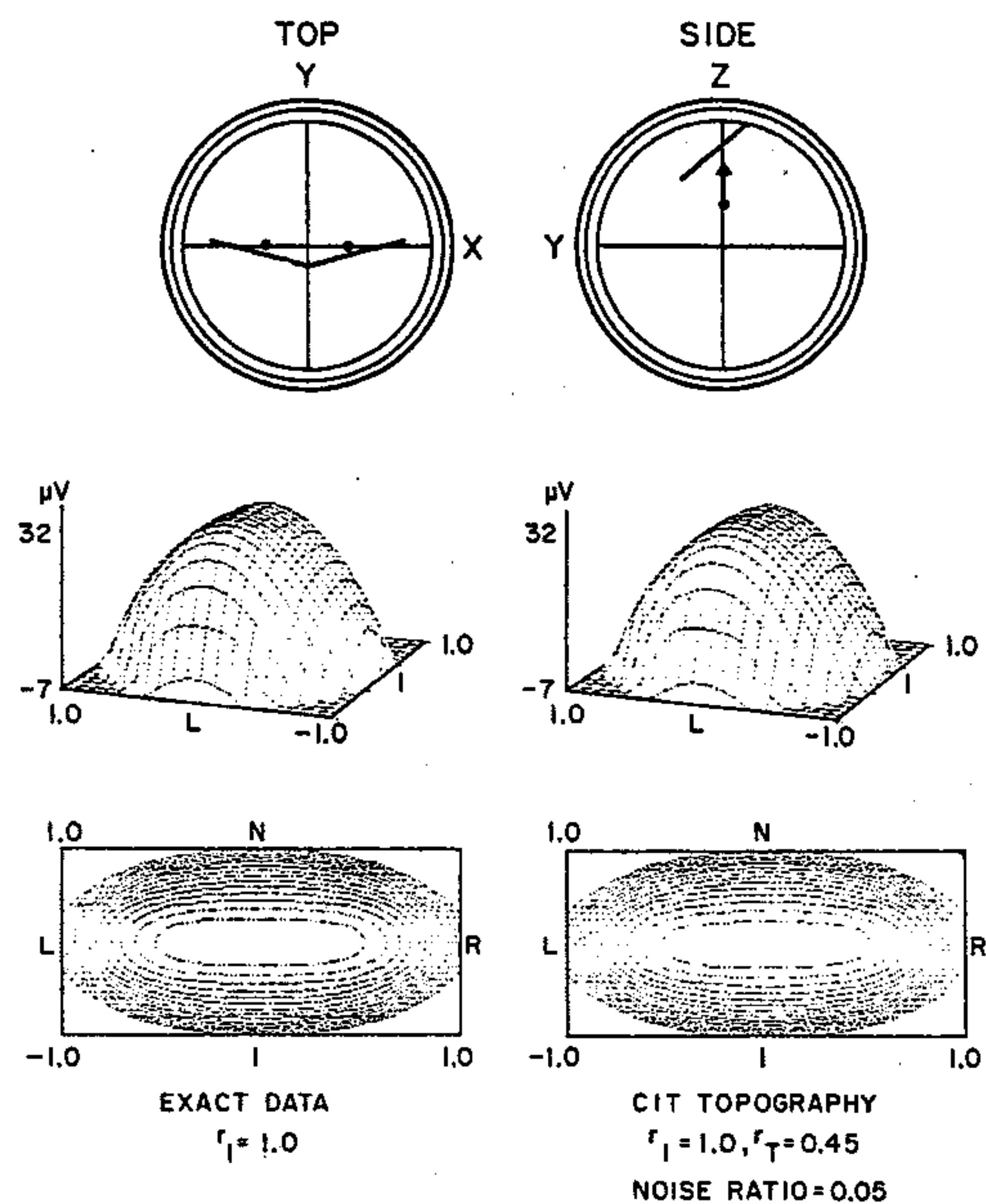


Fig. 2. The top row of figures shows the pair of dipole sources that are used to generate artificial data in the "head." The x axis passes through the right ear, the y axis passes through the nasion, and the z axis passes through the vertex. The heavy lines show the approximate location of the central fissure and the layers represent the brain, skull, and scalp. In this and subsequent figures: L = left ear, R = right ear, N = nasion, and I = inion. The maximum relative error was 0.02.

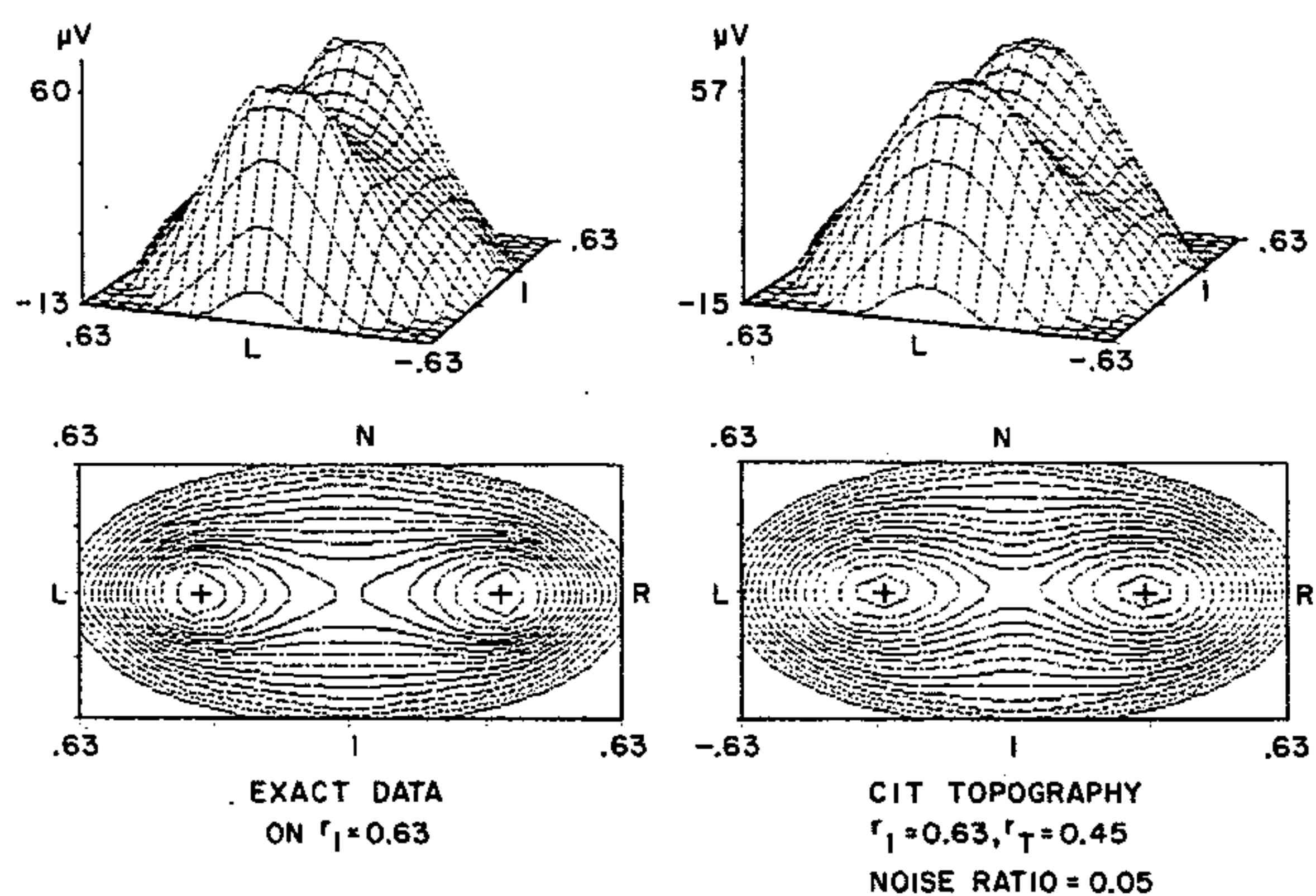


Fig. 3. Exact data and CIT-generated potential maps on an internal surface of radius 0.63 for the sources depicted in Fig. 2. The maximum relative error was 0.13.

10% of the maximum magnitude of the original data set). In this case the image surface is $r_I = 0.57$. Again the dipole pair is clearly distinguished.

Fig. 5 shows a final test of CIT on artificially generated data. The pair of dipole sources in this test is

$$(\pm 0.2 \sin(\pi/4), 0, 0.2 \cos(\pi/4), 0, 0, 0.1).$$

These sources lie on a spherical shell of radius 0.2 and are very close to one another. In this case the test surface $r_T = 0.3$, so that the dipole layer lies close to the actual sources. The image surface is the shell $r_I = 0.4$. If the noise ratio is taken to be 0.05, the effective rank of the system is 10 and the sources are not separated.

However, when the noise ratio is 0.001 the effective rank is 25 and the sources are clearly distinguishable. Note that this is the rank of the system obtained by ignoring singular values which are less than 0.001 times the maximum singular value.

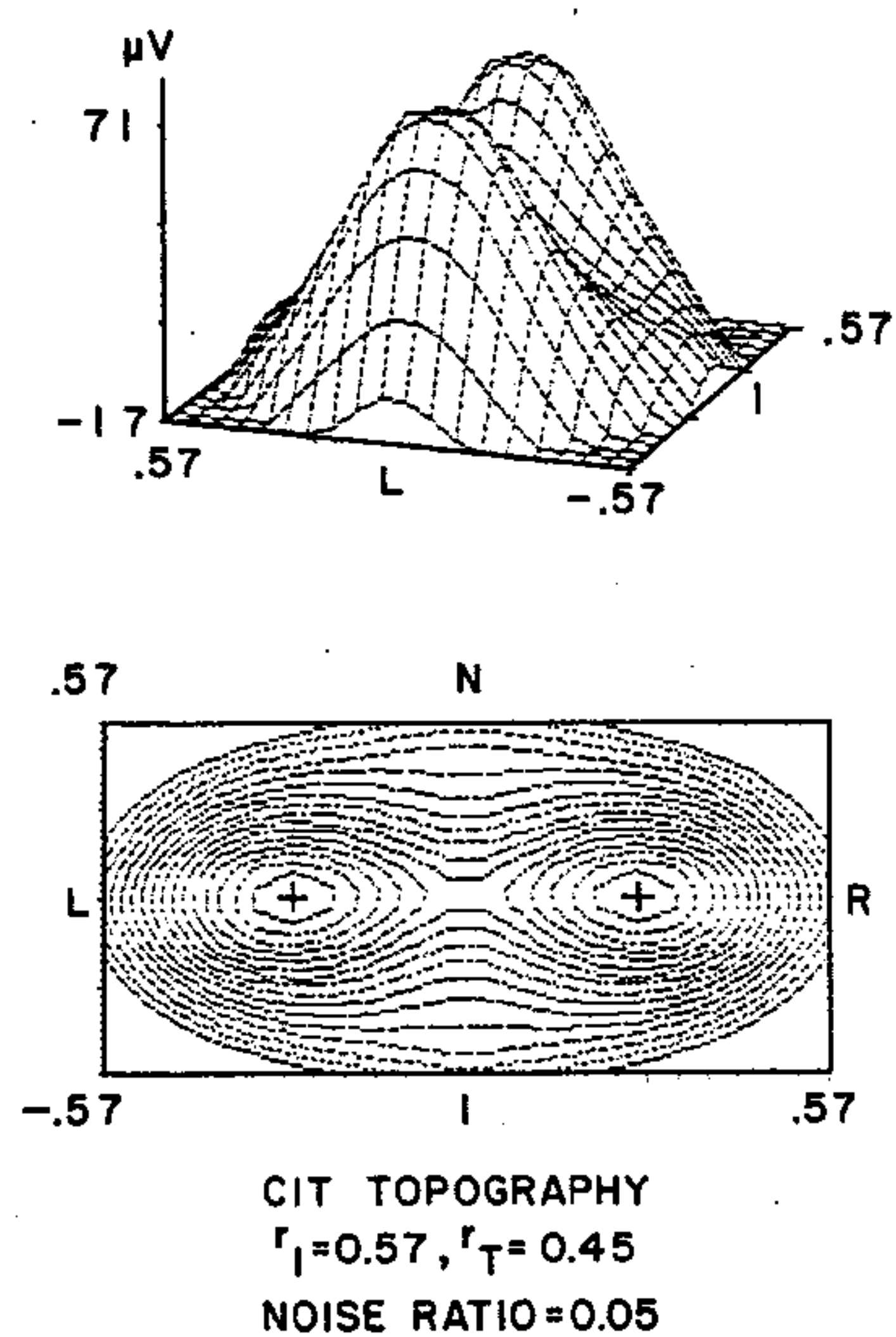


Fig. 4. CIT-generated potential map on surface of radius 0.57 when 10% noise is added to the surface data produced by the source pair in Fig. 2. The maximum relative error was 0.25.

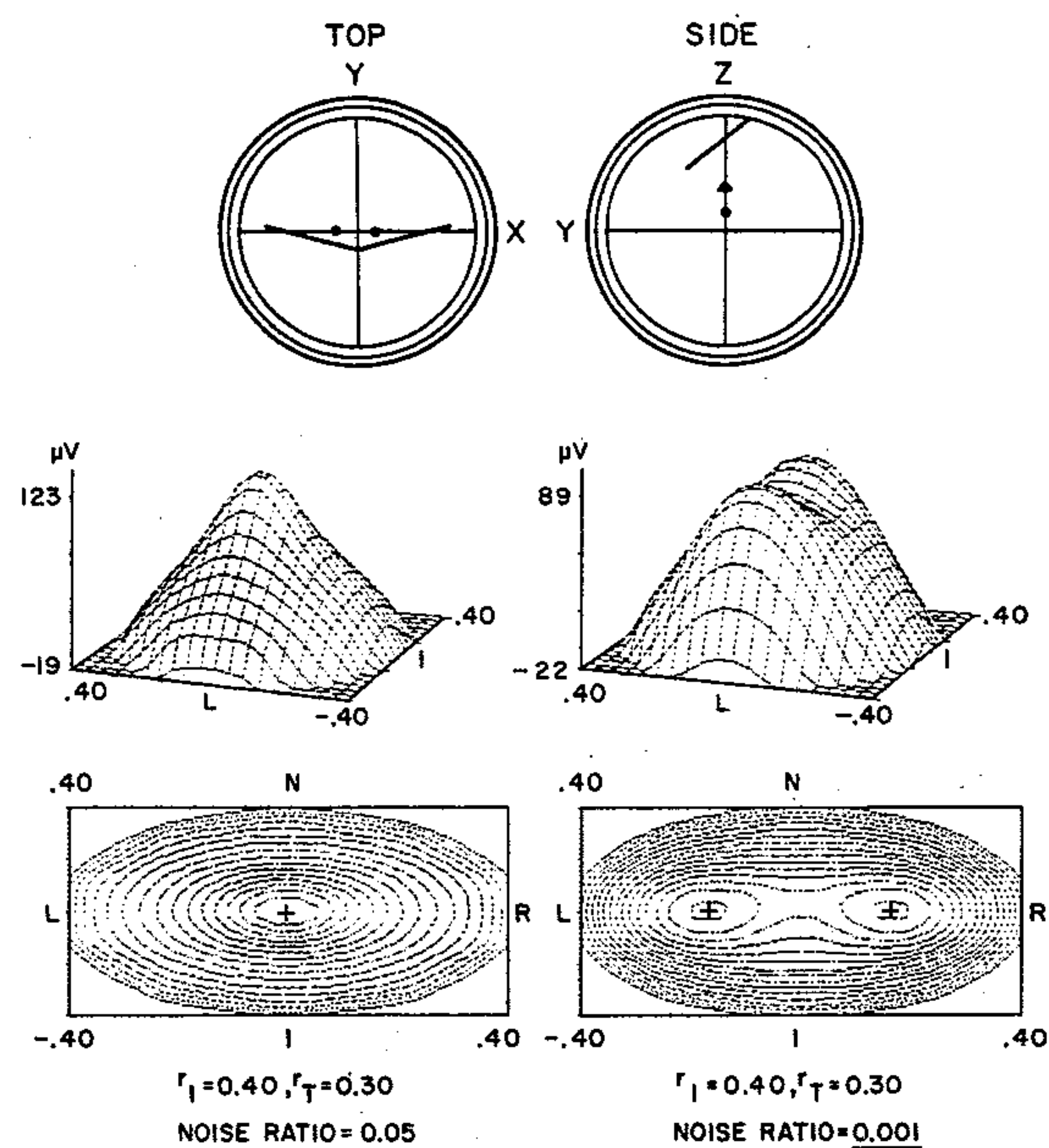


Fig. 5. The top row of figures shows the pair of dipole sources that are used to generate artificial data in the "head." These sources are closely spaced. The CIT-generated potential maps show two attempts to separate the source pair. The difference between these attempts is the choice of noise ratio in the SVD algorithm. The maximum relative error when the noise ratio is 0.05 is 0.52; when the noise ratio is 0.001 the maximum relative error is 0.11.

APPLICATIONS OF CIT TO EXPERIMENTAL DATA

Median Nerve Stimulation

The N30-P30 response to median nerve stimulation is probably generated in a localized area of the sensory cortex [4] and, as such, it is a useful test of CIT. The following application is to data furnished by C. C. Wood, Neuropsychology Laboratory of the West Haven (CT) Veterans Administration Medical Center.

CIT is applied to the response to "simultaneous" bilateral median nerve stimulation of a patient with a large left occipital-parietal tumor. This data was obtained by averaging the separate responses to left and right median nerve stimulation.

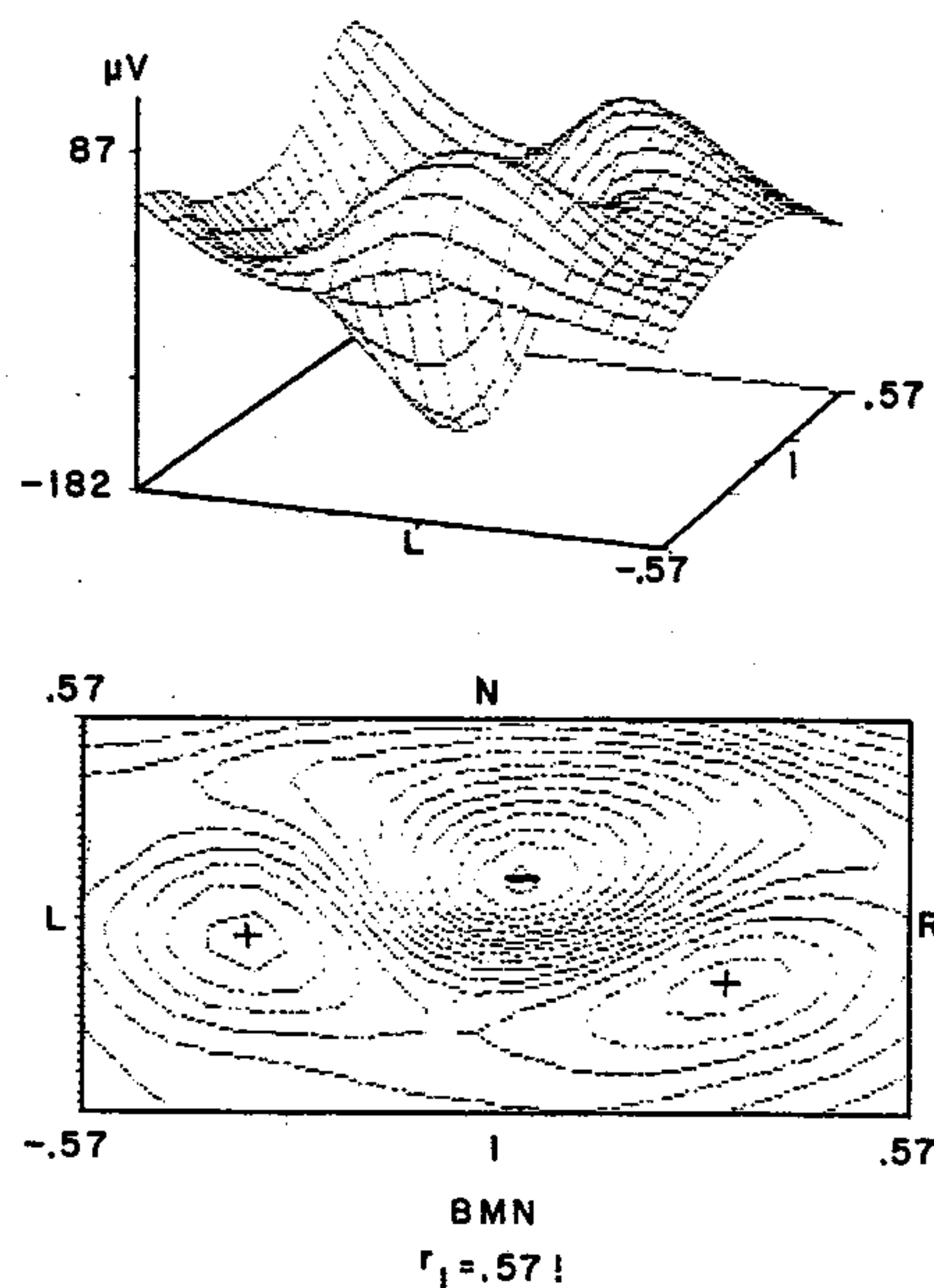


Fig. 6. Three-dimensional perspective and contour map generated by CIT for the response to bilateral median nerve stimulation 30 ms post-stimulus. $r_T = 0.45$, $r_l = 0.57$, noise ratio = 0.05.

In preparing Fig. 6, $r_T = 0.45$, $r_l = 0.57$, and the noise ratio is 0.05. This contour map suggests two superficial sources oriented tangentially to the surface of the brain. The asymmetry of the contours is compatible with the displacement of left sensory cortex by the tumor.

Pattern-Reversal Visual Stimulation

This final application of CIT is to the response to pattern-reversing visual stimulation in a normal volunteer. This data was furnished by M. R. Ford, Psychophysiology Laboratory of the Institute of Living, Hartford, CT. These results are for the N_2 component of the response, which presumably arises in layers of the striate cortex [8]. The first pair of figures gives the topographical contour map of the data. Subsequent figures are CIT generated topographies on layers of different radii in the spherical medium simulating the head. In each of these cases the test surface (on which the dipoles D_1, \dots, D_{160} lie) is $r_T = 0.45$, and the noise ratio is 0.05. The image surfaces are $r_l = 0.90$, 0.70, 0.57, in Fig. 7, and $r_l = 0.46$ in Fig. 8.

Each figure shows the extended surface-negative area over the occipital pole. This is consistent with the presumed origin of these potentials. As the image radius is decreased new details begin to appear in the contour maps—in this case there appears to be a low amplitude centric source that generates a surface-positive contribution at the vertex.

If one moves too close to the surface on which the test dipoles lie the contour maps lose detail. This occurs because the formulas which are used to calculate these maps (see Appendix) become infinite when a recording site on $r = r_l$ approaches one of the test dipoles on $r = r_T$.

DISCUSSION

The cortical imaging technique, by solving a harmonic inward continuation problem, appears to extract information from scalp-recorded electric potentials that is not apparent in conventional scalp topographical contour maps. For example, in applications of CIT to the artificial data generated by closely

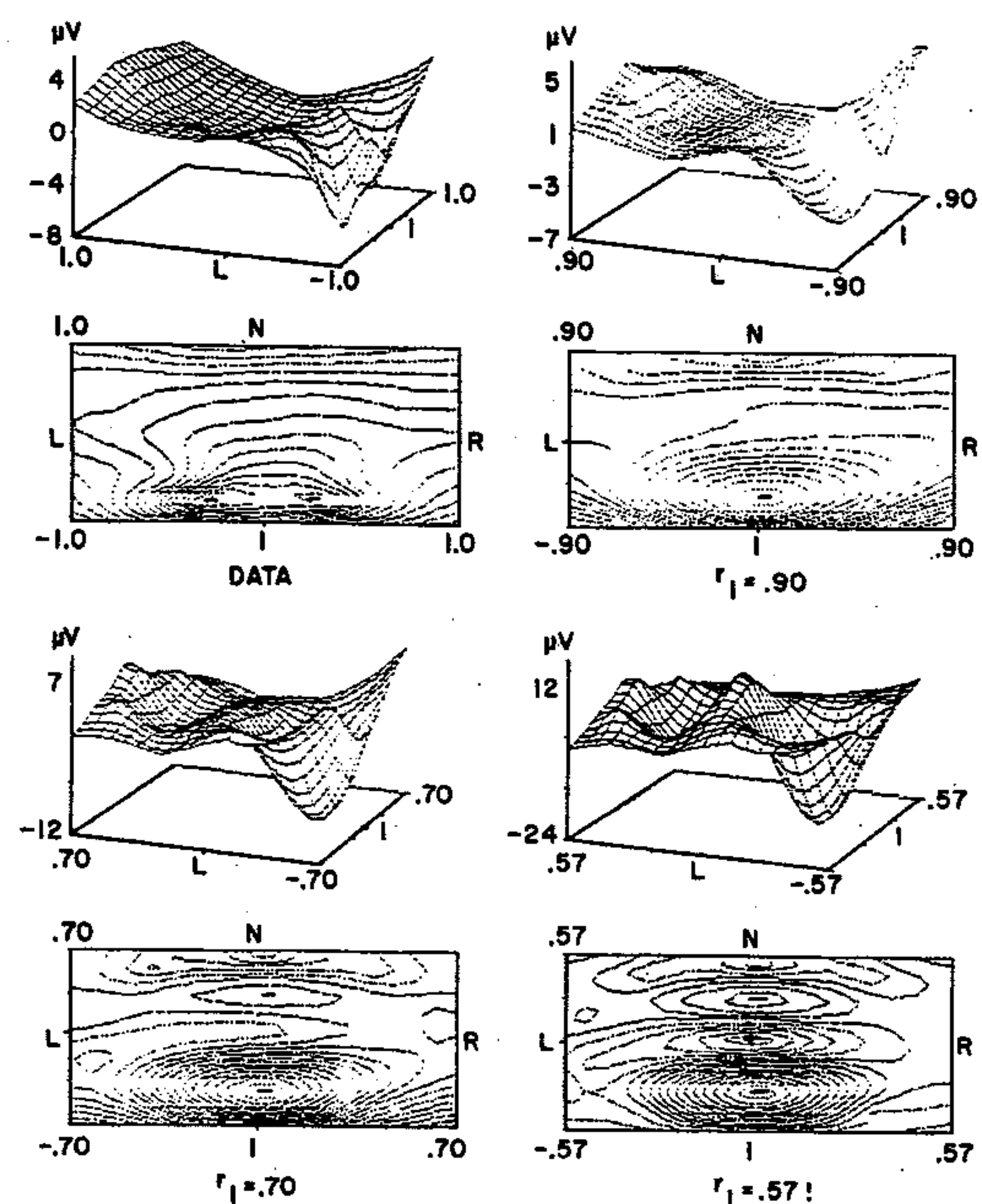


Fig. 7. Scalp data and CIT-generated potential maps for the N_2 response to pattern-reversal visual stimulation. $r_T = 0.45$, noise ratio = 0.05.

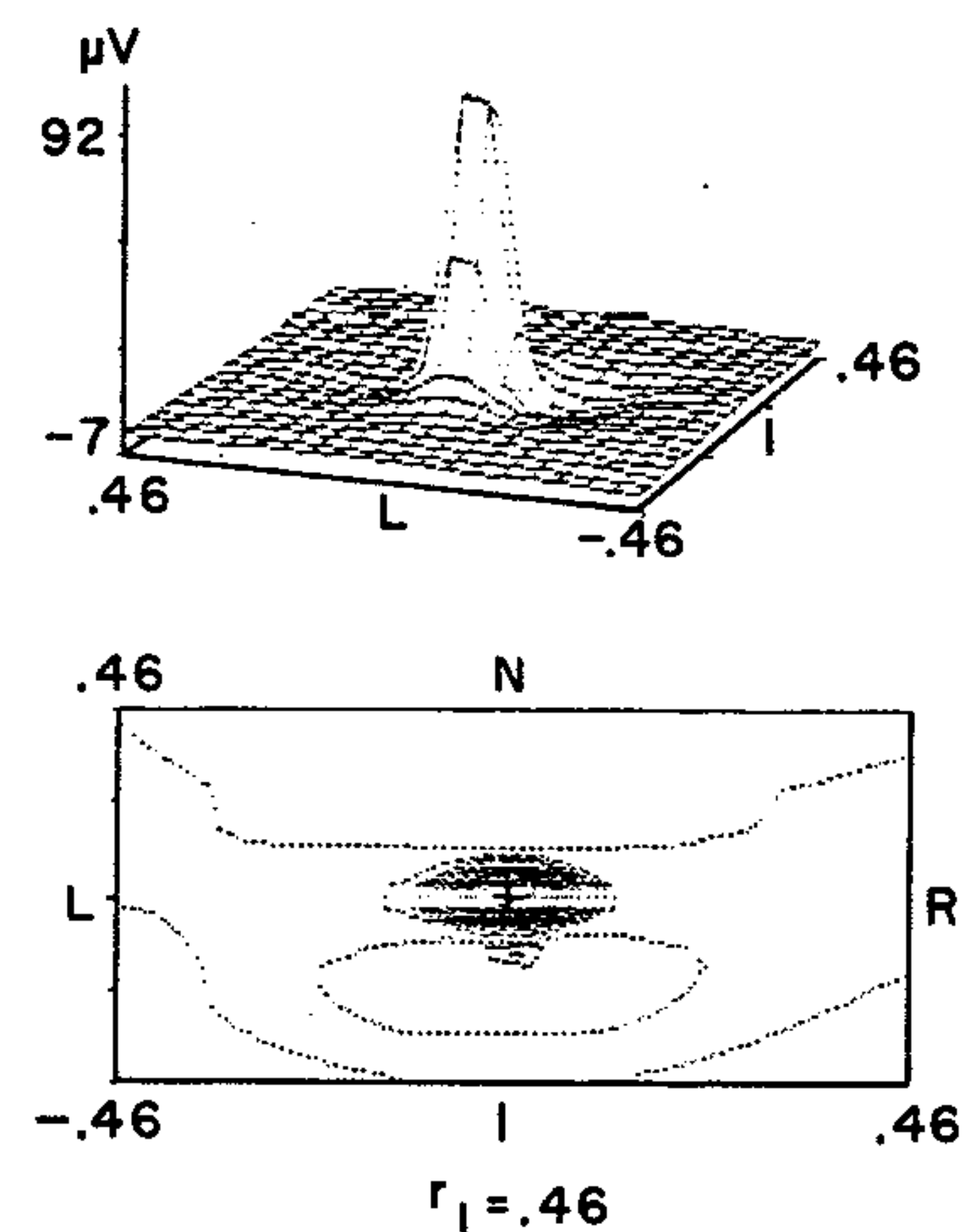


Fig. 8. CIT-generated potential map for the data in Fig. 7. The image surface $r_l = 0.46$ is very close to the test surface $r_T = 0.45$.

spaced pairs of dipoles, the method was able to discriminate multiple sources when surface topographical maps could not, even when noise was added to simulate the variability of measured potentials that would be observed in practice.

Applications of CIT to scalp-recorded potentials suggest that it might be possible to draw inferences about the neural generators of these potentials. For example, although correlations do exist between certain evoked waveforms or their topographical distributions on the one hand, and certain states of consciousness or abnormal brain activity on the other, these correlations are usually limited to inferences derived from the latencies or amplitudes of a few replicable EP components. The dipole localization method (DLM) appears to be sensitive in distinguishing between normal and abnormal responses and CIT suggests why a DLM result is abnormal—such as multiple or extended neural generators or generators whose location and/or orientation do not coincide with the location and orientation of the presumed neural sources of the potentials [1].

In the implementation of CIT, 160 radially oriented dipole of unit strength were placed on a "test" surface $r = r_T$. In most of our applications we found empirically that $r_T = 0.45$, in the unit sphere simulating the head, was the most effective depth to place the test dipoles. Also, in most cases, a noise ratio of 0.05 was used in the SVD program. With these parameters fixed, "cortical" images on surfaces with radii in the range $0.57 \leq r_I \leq 0.63$ most effectively brought out details concerning underlying physiological sources of scalp-recorded potentials. This layer is equivalent to a layer that approximates the surface of the "brain" in the model of the head consisting of three concentric layers [3], [9].

Although these initial experiments are very encouraging there is inherent uncertainty in computing hypothetical solutions to inverse problems by postulating the form of sources. Additional experimentation and tuning of the algorithm, along with comparison with actual depth-recorded data, will reveal precisely how closely the images that CIT generates approximate actual potential fields.

APPENDIX

In implementing CIT it is necessary to calculate the values of $V(D, P)$, the potential generated by the unit strength current dipole D on the test surface $r = r_T$ at the point P , which is on the image surface $r = r_I$. If γ is the angle between \overline{OD} and \overline{OP} , then equation (18) in [16] yields

$$V(D, P) = K \left[\frac{r_I \cos \gamma - r_T}{(r_I^2 + r_T^2 - 2r_I r_T \cos \gamma)^{3/2}} + \frac{r_I \cos \gamma - r_I^2 r_T}{(1 + (r_I r_T)^2 - 2r_I r_T \cos \gamma)^{3/2}} + \frac{1}{r_T(1 + (r_I r_T)^2 - 2r_I r_T \cos \gamma)^{1/2}} - \frac{1}{r_T} \right]. \quad (2)$$

If the dipole D is arbitrary, at location (p_1, p_2, p_3) , with moments m_1, m_2, m_3 , and $P = P(a_1, a_2, a_3)$ lies on the surface of the unit sphere then the following formula from [17] can be used:

$$V(D, P) = K \sum_{i=1}^3 \frac{m_i}{q_0} \left[\frac{2(a_i - p_i)}{q_0^2} + a_i + \frac{a_i s - p_i}{q_0 + 1 - s} \right] \quad (3)$$

where

$$q_0 = \left(\sum_{j=1}^3 (a_j - p_j)^2 \right)^{1/2}$$

and

$$s = \sum_{j=1}^2 a_j p_j.$$

So (3) can be used to generate artificial data on the surface of the sphere. The constant K depends upon the conductivity of the homogeneous sphere simulating the head. In this paper it is set equal to 1.

In any application of CIT to artificial or measured data, once the weighting parameters u_1, \dots, u_{160} have been calculated, it is easy to compute $\sum_{i=1}^{160} u_i V(D_i, P)$, using (2), to get the potential generated by the "optimal test layer of dipoles" at the point P .

In those cases when one needs to calculate $V(D, P)$ for arbitrary D and point P inside the sphere simulating the head, the

full equation (18) in [16] can be used. Finally, in order to find the optimal dipole source in the three-layer model of the head one can correct the location and moment parameters of the homogeneous sphere dipole using the correction factors in [3] or [9].

REFERENCES

- [1a] C. D. Hill, R. B. Kearfott, and R. D. Sidman, "The inverse problem of electroencephalography using an imaging technique for simulating cortical surface data," in *Proc. 12th IMACS World Cong.*, R. Vichnevetsky, P. Borne, J. Vignes, Eds., vol. 3, 1988, pp. 735-738.
- [1b] R. D. Sidman, R. B. Kearfott, D. J. Major, C. D. Hill, M. R. Ford, D. B. Smith, L. Lee, and R. Kramer, "Development and application of mathematical techniques for the noninvasive localization of the sources of scalp-recorded electric potentials," in *Biomed. Syst. Model. Simulation*, in *IMACS Trans. Scientific Computing*, vol. 5, J. Eisenfeld and D. S. Levine Eds. Basel: J. C. Baltzer AG, 1989, pp. 133-157.
- [2] R. D. Sidman, R. B. Kearfott, M. R. Ford, and C. Schlichting, "Analysis of normal and abnormal auditory and visual evoked responses using the dipole localization method and a new imaging technique (abstract)," *J. Clin. Neurophysiol.*, vol. 5, no. 4, p. 347, 1989.
- [3] J. P. Ary, S. A. Klein, and D. H. Fender, "Location of sources of evoked scalp potentials: Corrections for skull and scalp thicknesses," *IEEE Trans. Biomed. Eng.*, vol. 28, pp. 447-452, 1981.
- [4] R. D. Sidman, "The time-dependent equivalent dipole source for the response to median nerve stimulation," *IEEE Trans. Biomed. Eng.*, vol. 31, no. 6, pp. 481-483, 1984.
- [5] D. B. Smith, R. D. Sidman, J. S. Henke, D. Labiner, and H. Flanigin, "A reliable method for localizing deep intracranial sources of the EEG," *Neurol.*, vol. 35, no. 12, pp. 1702-1707, 1985.
- [6] L. Lee, D. B. Smith, R. D. Sidman, and R. Kramer, "Intracranial localization of epileptic spikes using DLM (abstract)," *J. Clin. Neurophysiol.*, vol. 5, no. 4, p. 336, 1988.
- [7] R. D. Sidman and D. B. Smith, "Photic stimulation to detect focal brain dysfunction," *Innovation et Technologie en Biologie et Medecine*, vol. 7, no. 3, pp. 323-330, 1986.
- [8] A. Ducati, E. Fava, and E. Motti, "Neuronal generators of the visual evoked potentials: Intracerebral recording in awake humans," *Electroencephalogr. clin. Neurophysiol.*, vol. 71, pp. 89-99, 1988.
- [9] M. Scherg and D. von Cramon, "Two bilateral sources of the late AEP as identified by a spatio-temporal dipole model," *Electroencephalogr. clin. Neurophysiol.*, vol. 62, pp. 32-44, 1985.
- [10] F. Richer, C. Alain, A. Achim, G. Bouvier, and J. Saint-Hilaire, "Intracerebral amplitude distributions of the auditory evoked potential," *Electroencephalogr. clin. Neurophysiol.*, vol. 74, pp. 202-208, 1989.
- [11] C. C. Wood, G. McCarthy, N. K. Squires, H. G. Vaughan, D. L. Woods, and W. C. McCallum, "Anatomical and physiological substrates of event-related potentials: Two case studies," *Ann. NY Acad. Sci. Brain Inform.: Event-related Potentials*, Karrer, Cohen, and Tueting, Eds., vol. 425, pp. 681-721, 1984.
- [12] J. R. Cannon, "Some numerical results for the solution of the heat equation backward in time," in *Numerical Solutions of Nonlinear Differential Equations*, D. Greenspan, Ed. New York: Wiley, 1967, pp. 21-54.
- [13] J. Douglas, "A numerical method for analytical continuation," in *Boundary Value Problems in Differential Equations*. Madison, WI: Univ. Wisconsin Press, 1960, pp. 179-189.
- [14] J. R. Cannon and J. Douglas, "The approximation of harmonic and parabolic functions on half-spaces from interior data," *CIME 20, Edizioni Cremonese*, pp. 193-230, 1967.
- [15] K. Miller, "Least squares methods for ill-posed problems with a prescribed bound," *SIAM J. Math. Anal.*, vol. 1, no. 1, pp. 52-74, 1970.
- [16] F. N. Wilson and R. H. Bayley, "The electric field of an eccentric dipole in a homogeneous spherical conducting medium," *Circulation*, vol. 1, pp. 84-92, 1950.
- [17] D. A. Brody, F. H. Terry, and R. E. Ideker, "Eccentric dipole

in a spherical medium: Generalized expression for surface potentials," *IEEE Trans. Biomed. Eng.*, vol. 20, pp. 141-143, 1973.

- [18] G. W. Stewart, *Introduction to Matrix Computations*. New York: Academic, 1973, pp. 317-326.
- [19] J. J. Dongarra, C. B. Moler, J. R. Bunch, and G. W. Stewart, "LIN-PACK users' guide," *SIAM*, Philadelphia, 1979.
- [20] G. H. Golub and C. F. van Loan, *Matrix Computations*, 2nd ed. Baltimore, MD: Johns Hopkins Univ. Press, 1989.



R. Baker Kearfott received the Ph.D. degree in mathematics from the University of Utah, Salt Lake City, in 1977.

He has been on the faculty at the University of Southwestern Louisiana since then. He spent a two-year leave of absence while serving in Computer and Information Support at Exxon Research and Engineering in Annandale, NJ. His general research interests include the numerical analysis of nonlinear algebraic systems, global optimization, interval analysis,

roundoff error analysis, and reliable computation, as well as scientific software development and biomedical and chemical kinetic modeling.



Robert D. Sidman received the Ph.D. degree in applied mathematics from Rensselaer Polytechnic Institute, Troy, NY, in 1968.

He has been on the faculty at the University of Southwestern Louisiana since 1974. He has been interested in the inverse problem of electroencephalography for nearly twenty years and his research has been supported by NIH, ASEE-ONR, Good Samaritan Hospital and The Institute of Living.

Dr. Sidman is a Fellow of the American EEG

Society.



Diana Joan Major received two B.S. degrees and two M.S. degrees in mathematics and physics from the University of Southwestern Louisiana.

She is currently enrolled in the Ph.D. program in mathematics and is writing her dissertation under the direction of Dr. Sidman. She was awarded an Air Force Summer Research Fellowship to work on signal analysis at Wright Patterson Air Force Base in 1989. She also won the Caton Award, given by the Southern EEG

Society for the best pre-M.D. or pre-Ph.D. paper on electrophysiology, and she has delivered papers at national biomedical and mathematical meetings.



C. Denson Hill received the B.S. degree in mathematics and physics from Rice University, Houston, TX, in 1961 and the Ph.D. degree in mathematics from the Courant Institute, New York University, New York City, in 1966.

He is Professor of Mathematics at State University of New York at Stony Brook. His main interests are in pure mathematics, in the fields of several complex variables, partial differential equations, and complex geometry; however his activities occasionally include applied

mathematics, in the areas of inverse problems, free boundary problems and nonlinear geometric optics.